Editors' Suggestion | Featured in Physics

Positronium Laser Cooling via the 1^3S-2^3P Transition with a Broadband Laser Pulse

L. T. Glöggler,[1] N. Gusakova,[1,2] B. Rienäcker,[3,*] A. Camper,[4,†] R. Caravita,[5,‡] S. Huck,[1,6] M. Volponi,[1,7,5] T. Wolz,[1] L. Penasa,[7,5] V. Krumins,[1,8] F. P. Gustafsson,[1] D. Comparat,[9] M. Auzins,[8] B. Bergmann,[10] P. Burian,[10] R. S. Brusa,[7,5] F. Castelli,[11,12] G. Cerchiari,[13] R. Ciuryło,[14] G. Consolati,[11,15] M. Doser,[1] Ł. Graczykowski,[16] M. Grosbart,[1] F. Guatieri,[7,5] S. Haider,[1] M. A. Janik,[16] G. Kasprowicz,[17] G. Khatri,[1] Ł. Kłosowski,[14] G. Kornakov,[16] L. Lappo,[16] A. Linek,[14] J. Malamant,[4] S. Mariazzi,[7,5] V. Petracek,[18] M. Piwiński,[14] S. Pospíšil,[10] L. Povolo,[7,5] F. Prelz,[11] S. A. Rangwala,[19] T. Rauschendorfer,[1,20] B. S. Rawat,[3,21] V. Rodin,[3] O. M. Røhne,[4] H. Sandaker,[4] P. Smolyanskiy,[10] T. Sowiński,[22] D. Tefelski,[16] T. Vafeiadis,[1] C. P. Welsch,[3,21] M. Zawada,[14] J. Zielinski,[16] and N. Zurlo[23,24]

(AEgIS Collaboration)

[1]*Physics Department, CERN, 1211 Geneva 23, Switzerland*
[2]*Department of Physics, NTNU, Norwegian University of Science and Technology, Trondheim, Norway*
[3]*Department of Physics, University of Liverpool, Liverpool L69 3BX, United Kingdom*
[4]*Department of Physics, University of Oslo, Sem Sælandsvei 24, 0371 Oslo, Norway*
[5]*TIFPA/INFN Trento, via Sommarive 14, 38123 Povo, Trento, Italy*
[6]*Institute for Experimental Physics, Universität Hamburg, 22607 Hamburg, Germany*
[7]*Department of Physics, University of Trento, via Sommarive 14, 38123 Povo, Trento, Italy*
[8]*University of Latvia, Department of Physics Raina boulevard 19, LV-1586 Riga, Latvia*
[9]*Université Paris-Saclay, CNRS, Laboratoire Aimé Cotton, 91405 Orsay, France*
[10]*Institute of Experimental and Applied Physics, Czech Technical University in Prague, Husova 240/5, 110 00 Prague 1, Czech Republic*
[11]*INFN Milano, via Celoria 16, 20133 Milano, Italy*
[12]*Department of Physics "Aldo Pontremoli," University of Milano, via Celoria 16, 20133 Milano, Italy*
[13]*Institut für Experimentalphysik, University of Innsbruck, Technikerstrasse 25, 6020 Innsbruck, Austria*
[14]*Institute of Physics, Faculty of Physics, Astronomy, and Informatics, Nicolaus Copernicus University in Torun, Grudziadzka 5, 87-100 Torun, Poland*
[15]*Department of Aerospace Science and Technology, Politecnico di Milano, via La Masa 34, 20156 Milano, Italy*
[16]*Warsaw University of Technology, Faculty of Physics, ul. Koszykowa 75, 00-662 Warsaw, Poland*
[17]*Warsaw University of Technology, Faculty of Electronics and Information Technology, ul. Nowowiejska 15/19, 00-665 Warsaw, Poland*
[18]*Czech Technical University, Prague, Brehova 7, 11519 Prague 1, Czech Republic*
[19]*Raman Research Institute, C. V. Raman Avenue, Sadashivanagar, Bangalore 560080, India*
[20]*Felix Bloch Institute for Solid State Physics, Universität Leipzig, 04103 Leipzig, Germany*
[21]*The Cockcroft Institute, Daresbury, Warrington WA4 4AD, United Kingdom*
[22]*Institute of Physics, Polish Academy of Sciences, Aleja Lotnikow 32/46, PL-02668 Warsaw, Poland*
[23]*INFN Pavia, via Bassi 6, 27100 Pavia, Italy*
[24]*Department of Civil, Environmental, Architectural Engineering and Mathematics, University of Brescia, via Branze 43, 25123 Brescia, Italy*

(Received 13 October 2023; accepted 18 January 2024; published 22 February 2024)

We report on laser cooling of a large fraction of positronium (Ps) in free flight by strongly saturating the 1^3S-2^3P transition with a broadband, long-pulsed 243 nm alexandrite laser. The ground state Ps cloud is produced in a magnetic and electric field-free environment. We observe two different laser-induced effects. The first effect is an increase in the number of atoms in the ground state after the time Ps has spent in the long-lived 2^3P states. The second effect is one-dimensional Doppler cooling of Ps, reducing the cloud's temperature from 380(20) to 170(20) K. We demonstrate a 58(9)% increase in the fraction of Ps atoms with $v_{1D} < 3.7 \times 10^4$ ms^{-1}.

DOI: 10.1103/PhysRevLett.132.083402

Positronium (Ps), discovered in 1951, is the lightest known atomic system, consisting only of an electron (e^-) and a positron (e^+) [1]. Ps has been extensively studied for its exotic properties as a purely leptonic matter-antimatter system. So far, experiments researching Ps have relied on formation processes that result in clouds with a large velocity distribution, in the order of several 10^4 ms^{-1} [2–4]. This, for instance, has been limiting the precision of spectroscopy studies due to the large Doppler broadening of the transition lines [5,6]. The idea of using laser cooling to narrow the Ps velocity distribution dates back to 1988 [7], following the first demonstration of laser cooling on neutral atoms by just a few years [8]. Despite significant efforts [9], Ps laser cooling has not been experimentally achieved yet. A whole range of new fundamental experiments would become feasible with a sufficient amount of cold Ps [10,11]. These include 1^3S-2^3S precision spectroscopy at the 100 kHz level, which will enable testing bound state QED at the $\alpha^7 m_{e^+}$ order [12], measuring the m_{e^+}/m_{e^-} mass ratio with unprecedented accuracy [13], and testing the equivalence principle (EP) with a purely leptonic system by looking at the transition redshift around the Sun's orbit [14]. Testing the EP with atomic systems consisting of antimatter is the primary goal of AEgIS, building on the availability of cold Ps for efficient Rydberg antihydrogen ($\bar{H}^*$) production through the charge exchange reaction $Ps^* + \bar{p} \rightarrow \bar{H}^* + e^-$ between cold antiprotons ($\bar{p}$) and Rydberg-excited Ps (Ps^*) [15,16]. This reaction's efficiency can be significantly increased by reducing the temperature of the Ps^* cloud [17]. Moreover, forming a Ps Bose-Einstein condensate (BEC) [10,18] would allow studying stimulated annihilation, producing coherent light in the γ radiation range [19,20]. This objective (plus precision spectroscopy) is being pursued by the UTokyo group [21], which is actively developing Ps laser cooling with a chirped laser pulse [22].

Here, we report on the first experimental demonstration of Ps laser cooling by strongly saturating the 1^3S-2^3P transition [Fig. 1(a)] for 70 ns, employing an alexandrite-based laser system developed specifically to meet these requirements: high intensity, large bandwidth, and long pulse duration. The velocity distributions with and without laser cooling were obtained by Doppler-sensitive two-photon resonant ionization along the 1^3S-3^3P transition [3] [Fig. 1(a)].

Ps is produced by implanting e^+ bunches with 3.3 keV energy into a nanochanneled silicon converter [4,23]. This e^+/Ps converter has a Ps yield of about 30%, corresponding to a few 10^5 Ps per bunch. It is mounted at a 45° angle with respect to the e^+ beam axis, as shown in Fig. 1(b). Typically, both e^+ beam and emitted Ps cloud are about 5 mm in diameter. All experiments are conducted in a magnetic and electric field-free environment. An electrostatic buncher [24] with fast potential switch off [25] and a μ-metal shield are used to minimize residual fields. A low residual magnetic field, measured to be below 1 mT in the

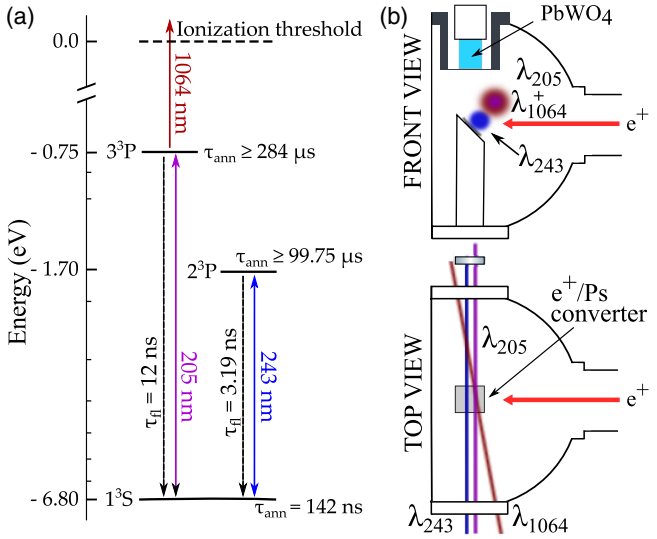

FIG. 1. Experimental layout for Ps laser cooling. (a) Diagram of relevant Ps energy levels and transitions, highlighting transition wavelengths and annihilation or fluorescence lifetimes. (b) Front and top view of the vacuum setup, featuring the cooling (λ_{243}) and the two probing lasers (λ_{205} and λ_{1064}), the $PbWO_4$ detector, and the dichroic mirror used to selectively retroreflect the cooling beam.

Ps production area, is important toward Ps laser cooling, as in intermediate magnetic field ranges the saturation of the 1^3S-2^3P transition leads to fast annihilation due to singlet-triplet state mixing in the excited state manifold [26]. This effect, called "magnetic quenching," prevents efficient cooling [27] and strongly encourages to work either in the Paschen-Back regime [28] or, as we do, in a magnetic field-free environment.

The Ps 1^3S-2^3P transition is driven by the third harmonic of a Q-switched alexandrite laser [29], as proposed in [10], whose main features are briefly summarized hereafter. The optical length of the cavity is 1 m. The pulse length of 70 ns, much longer than the spontaneous emission lifetime of the 1^3S-2^3P transition (3.19 ns), allows several cooling cycles per pulse [10]. The central wavelength is set by an intracavity volume Bragg grating (VBG) [30]. Rotating the VBG finely tunes the fundamental wavelength with an absolute accuracy of 10 pm. Two lithium triborate (LBO) crystals and two β-barium borate (BBO) crystals are used to generate up to 2.3 mJ at the third harmonic. At 243 nm, the measured root-mean-square (rms) spectral bandwidth is $\sigma_{243} = 101(3)$ GHz. The laser [29] was specifically designed to deliver an irradiance of 100 kW cm^{-2} when focusing 0.7 mJ on an area of 10 mm^2. As a result, the power on the 20 MHz rms resonance transition linewidth amounts to $100\,\mathrm{kW\,cm^{-2}} \times 20\,\mathrm{MHz}/101\,\mathrm{GHz} = 20\,\mathrm{W\,cm^{-2}}$, much higher than the saturation intensity of the 1^3S-2^3P transition of 0.45 W cm^{-2} [27]. The laser fluence fills in the spectral gaps in the laser bandwidth [31] and the population in the excited state is saturated within a 360(15) GHz large spectral

bandwidth. It should be noted that in these conditions less than 1% of the atoms are photoionized [27]. The transverse Doppler profile was probed by fine-tuning the wavelength of a 1.5-ns-long 205 nm pulse with an rms spectral bandwidth of $\sigma_{205} = 179(9)$ GHz or 25(1) pm, populating the 3^3P states. A 4-ns-long 1064 nm pulse synchronized with the 205 nm pulse induced photoionization of the excited states [32].

The Pockels cell of the alexandrite laser cavity is connected to a high-voltage (HV) electronic switch, which opens and closes the cavity with nanosecond precision to generate a Q-switched pulse featuring a controllable sharp falling edge. Consequently, the laser emission can be suppressed imminent to the arrival of the 205 nm pulse probing the velocity profile, avoiding a temporal overlap of the cooling and probing laser pulses. The 205 nm pulse interacts with Ps about 12 ns after the 243 nm pulse has subsided. This ensures that the transiently excited Ps have spontaneously decayed to the ground state before probing the velocity distribution of the cloud. Nanosecond synchronization between laser pulses, HV switch, and e^+ was realized by ARTIQ and Sinara control electronics [33] coordinated by a LabVIEW-based distributed control system [34]. The 243 nm laser beam is copropagating with the 205 nm pulse [Fig. 1(b)] and retroreflected by a dichroic mirror transmitting the 205 nm light. All laser beams are linearly polarized.

The time distribution of the γ radiation resulting from Ps annihilations, the so-called single-shot positron annihilation lifetime spectroscopy (SSPALS) [35] spectrum, was acquired in different laser configurations. As illustrated in Fig. 2, the configurations "no lasers," "205 nm + 1064 nm", "243 nm only," and "243 nm + 205 nm + 1064 nm" were used. A $25 \times 25 \times 25$ mm $PbWO_4$ scintillator placed 40 mm above the e^+/Ps converter, coupled to a Hamamatsu R11265-100 photomultiplier tube and a Teledyne LeCroy HDO4104A oscilloscope, was used to acquire SSPALS spectra [32].

The long tail in the SSPALS spectrum measured without lasers (black dotted curve), extending from 150 to 400 ns in Fig. 2, reflects the 142 ns lifetime of 1^3S Ps in vacuum. Firing the 243 nm laser only, a large fraction of Ps is excited to the 2^3P level, where the annihilation lifetime is much longer than in the ground state. Consequently, the annihilation rate at later times increases (green dash-dotted line in Fig. 2) due to an increase in the number of annihilating atoms in the ground state. By sending the 205 nm + 1064 nm pulses only, a fraction of the atoms is selectively photoionized. This leads to an immediate small increase in the γ emission as a fraction of the isotropically emitted photodissociated e^+ hits the conversion target and annihilates (small bump at 90 ns in Fig. 2), followed by a reduction of the number of ground state Ps annihilating with 142 ns lifetime (red dashed curve). The interaction of the Ps cloud with all three lasers induces a combined effect (blue solid curve in Fig. 2).

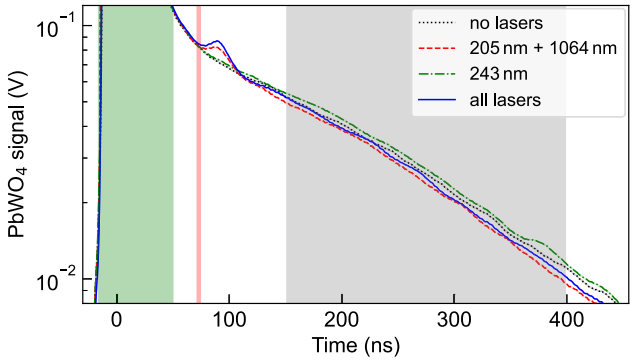

FIG. 2. SSPALS spectra of Ps in vacuum without lasers (black dotted curve), with the 205 nm + 1064 nm lasers (red dashed curve), with the 243 nm laser only (green dash-dotted curve), and with all three lasers 243 nm + 205 nm + 1064 nm (blue solid curve). The 243 nm laser is firing during the time window from −20 to 50 ns (green band), while the 205 nm + 1064 nm (red vertical line) are injected 75 ns after e^+ implantation time ($t = 0$ ns). Each curve is an average of 90 individual spectra. The statistical error is smaller than the linewidths. For analysis, the spectra were integrated between 150 and 400 ns (light gray area).

In order to study the effects caused by the different laser configurations, S parameters are constructed as

$$S = \frac{f_{\mathrm{ON}} - f_{\mathrm{OFF}}}{f_{\mathrm{OFF}}}, \tag{1}$$

where f_{ON} and f_{OFF} denote the integrated SSPALS spectra in the time window between 150 and 400 ns (gray band in Fig. 2). "ON" refers to laser(s) interacting with the Ps cloud, and "OFF" to no laser interaction. In the following, we will refer to $S_{205+1064}$ when only the probing lasers are present, and S_{243} when only the cooling laser is present. We further define S_{cool} as the difference between $S_{243+205+1064}$ (when all three lasers are present) and S_{243}:

$$S_{\mathrm{cool}} = S_{243+205+1064} - S_{243}. \tag{2}$$

S_{cool} reflects the number of photoionized Ps atoms by the probing laser after the interaction with the cooling laser, normalized by the number of Ps atoms annihilating in the absence of any laser. The S-parameter values are calculated by averaging over many sets of spectra acquired consecutively in all the above-mentioned laser configurations. A detrending procedure is applied [36] to correct for slow changes in the amount of Ps produced over time, caused by moderator aging during the long measurement period. A trend function is built by applying Gaussian radial basis regression [37] to the f_{OFF} dataset. Subsequently, S parameters are calculated by evaluating the trend function at exactly the time at which the SSPALS spectra with laser(s) are acquired.

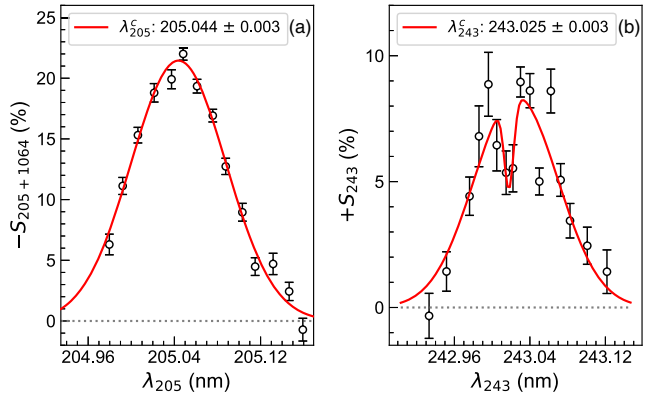

FIG. 3. Ps velocity distribution measured by SSPALS. (a) Transverse Doppler profile measured by two-photon resonant ionization. A Gaussian fit yields an rms width of 44(1) pm, which translates to a Ps rms velocity of $5.3 \pm 0.2 \times 10^4$ ms^{-1} after deconvoluting the σ_{205} laser bandwidth. (b) Velocity-resolved increase in the number of ground state Ps atoms, induced by the 243 nm transitory excitation to the 2^3P level. At resonance, the expected Lamb dip is observed. A 2-Gaussian fit yields an rms width of the enveloping Gaussian of 44(3) pm, which corresponds to a Ps rms velocity of $4.9 \pm 0.4 \times 10^4$ ms^{-1}.

First, the Ps velocity distribution without laser cooling was measured by scanning the λ_{205} detuning with the 205 and 1064 nm laser beams grazing the surface of the e^+/Ps converter. In this experiment, the laser pulses were fired 50 ns after the e^+ implantation time. The transverse Doppler profile [Fig. 3(a)] is fitted with a Gaussian function, yielding an rms width of 44(1) pm. This width corresponds to a Ps rms velocity of $5.3 \pm 0.2 \times 10^4$ ms^{-1} after deconvoluting the σ_{205} probing laser bandwidth. This rms velocity is associated with a transverse temperature of 370(30) K. The resulting line is centered at $\lambda^c_{205} = 205.044(3)$ nm, which is compatible with the theoretical value [32].

Second, we performed saturated absorption spectroscopy on the 1^3S-2^3P transition [38] to determine the center of the line and to characterize the effect of the cooling pulse on the SSPALS spectrum. Figure 3(b) displays the S_{243} parameter calculated from SSPALS spectra, recorded as a function of the λ_{243} detuning. The cooling laser pulse is synchronized with the e^+ implantation time (see Fig. 2). It is worth noting that the resulting S values are now positive, in contrast to what was observed in the two-photon resonant ionization experiment. To the best of our knowledge, such an increase in the number of ground state Ps atoms caused by a transitory laser excitation to the 2^3P level has never been observed and can be classified as a laser-induced, spectrally tunable preservation of Ps. This effect has the same physical origin as the one observed in the lifetime enhancement of Ps atoms excited to Rydberg states [31]. The observed line shape shows a Lamb dip, demonstrating the saturation of the 1^3S-2^3P transition by the laser [38]. A 2-Gaussian model is fitted to the data, following the approach taken in Ref. [38]. The transition line is centered at $\lambda^c_{243} = 243.025(3)$ nm, which is in agreement with previous measurements [38]. The enveloping Gaussian features an rms width of 44(3) pm, which corresponds to a Ps rms velocity of $4.9 \pm 0.4 \times 10^4$ ms^{-1} [320(50) K] after deconvoluting the σ_{243} cooling laser bandwidth.

With this understanding of the individual laser interactions with the Ps cloud, we then performed experiments combining the 243 nm cooling laser and the 205 nm + 1064 nm probing lasers. The cooling laser remains synchronized with the e^+ implantation time and in the same spatial position [Fig. 1(b), blue spot]. The probing laser pulse is delayed by 75 ns with respect to the positron implantation time [3,25] (red vertical line in Fig. 2) and moved to a position at a distance of 7 mm from the converter surface [Fig. 1(b), violet spot] corresponding to the distance covered by the atoms in the peak-velocity component of the axial velocity distribution during 70 ns. These parameters are chosen to reach a $S_{205+1064}$ of ~10% with the probing laser tuned at resonance. To characterize the change in the Ps velocity distribution induced by the cooling laser, the detuning of the 243 nm laser is set to −200 GHz (corresponding to $\lambda_{243} = 243.061$ nm) and a photoionization Doppler scan is performed. The S_{cool} parameter measured as a function of the detuning of the probing laser is shown in Fig. 4. The curve is compared to the $S_{205+1064}$ distribution measured in the same configuration (75 ns delay and 7 mm away from the e^+/Ps converter), but without prior interaction with the cooling laser. Both of the one-dimensional transverse Doppler profiles were obtained by applying a moving average to the ~350 single S values with a square window (350 GHz in width).

The one-dimensional transverse Doppler profile obtained in the presence of the 243 nm cooling laser is narrower than the one measured without it. The asymmetry of the two profiles is caused by a slight increase in the pulse energy of the 205 nm probing laser toward blue-detuned wavelengths. A simple Gaussian fit on each of the two distributions was used to quantify the change in the velocity profile. With cooling, we find an rms width of 269(1) GHz, in contrast to 330(2) GHz without cooling. After deconvoluting the standard deviation of the moving average window (350 GHz/$\sqrt{12}$) and the σ_{205} laser bandwidth, the Ps rms velocities corresponding to these widths are $5.4 \pm 0.2 \times 10^4$ ms^{-1}, associated with a temperature of 380(20) K, and $3.7 \pm 0.2 \times 10^4$ ms^{-1} associated with 170(20) K, respectively. The obtained rms velocity in the absence of the cooling laser is in agreement with the results reported in Fig. 3. The interaction with the 70-ns-long 243 nm laser pulse reduces the Ps rms velocity by $1.7 \pm 0.3 \times 10^4$ ms^{-1}, corresponding to a temperature reduction of $\Delta T = 210(30)$ K. The systematic error associated with the arbitrary choice of a Gaussian fitting model is estimated to be ±10 K.

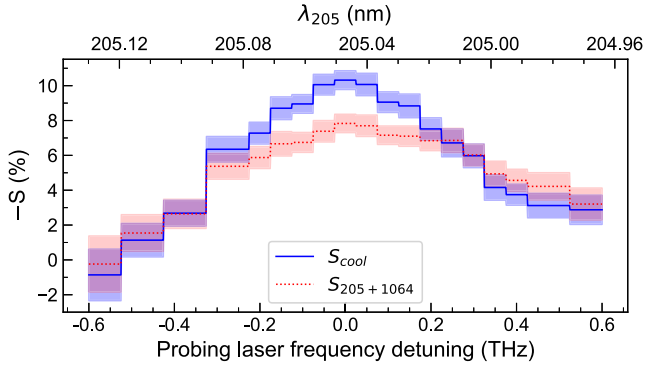

FIG. 4. One-dimensional transverse Doppler profiles of the Ps cloud with (solid curve) and without (dotted curve) interaction with the 243 nm cooling laser beam at a fixed frequency detuning of −200 GHz. The semitransparent bands represent the statistical measurement error (one standard deviation of the average).

Given the high optical intensity of the 243 nm laser, the average time for all addressed Ps atoms to undergo a single cooling cycle is 6.38 ns [10]. Consequently, a maximum of 11 cooling cycles can be reached within the 70-ns-long laser-Ps interaction. Since the recoil velocity for a single 1^3S-2^3P transition of Ps is $v_{\mathrm{recoil}} = 1.5 \times 10^3$ ms^{-1} [27], the velocity reduction can reach $11v_{\mathrm{recoil}} = 1.65 \times 10^4$ ms^{-1}, corresponding to a temperature reduction of about 200 K, in agreement with our measurements.

To evaluate the maximum fraction of fast Ps that can be pushed toward null velocity via recoil effect, the cooling laser detuning was scanned from −0.65 to 0.25 THz while the 205 nm laser remained at resonance. The result of this scan is shown in Fig. 5. The horizontal dashed line is the signal measured when only the probing laser interacts with the Ps cloud ($S_{205+1064}$), yielding $-S = 8.0(2)\%$ as the reference for the population near resonance. The blue curve is the S_{cool} parameter as defined in Eq. (2). The curve was obtained by applying a moving average with a window size of 200 GHz. For a given λ_{243} detuning, the difference between S_{cool} and $S_{205+1064}$ corresponds to the fraction of Ps atoms cooled within the bandwidth of the 205 nm laser, i.e., having velocities smaller than 3.7×10^4 ms^{-1}. The $-S$ value at −200 GHz detuning in Fig. 5 is compatible with that of Fig. 4 at resonance ($9.2 \pm 1.8\%$ and $10.4 \pm 0.5\%$, respectively). We find a maximum relative increase of 58(9)% at a detuning of −350 GHz.

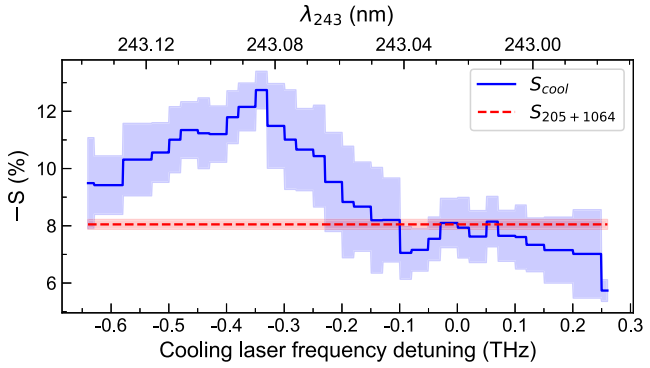

FIG. 5. Number of Ps atoms with $v_{1\mathrm{D}} < 3.7 \times 10^4$ ms^{-1}, as a function of the cooling laser frequency detuning, normalized to the number of Ps atoms in the absence of all lasers. The dashed horizontal line represents the reference population of Ps in this velocity range with the cooling laser off. The highest observed relative increase is 58(9)% at a cooling laser frequency detuning of −350 GHz. The semitransparent bands represent the statistical uncertainties (one standard deviation of the average).

In conclusion, we have experimentally demonstrated laser cooling of a large fraction of a thermal Ps cloud in a magnetic and electric field-free environment and reduced the velocity rms by $11v_{\mathrm{recoil}} = 1.65 \times 10^4$ ms^{-1} in 70 ns, which is the limit of the efficiency allowed by standard Doppler cooling. A temperature decrease from 380(20) to 170(20) K was observed. Our Letter also gives an in-depth understanding of the different laser-Ps interactions and their manifestation in the SSPALS spectra. In particular, we observed an increase in the number of ground state atoms after Ps has been transiently excited to the 2^3P states. Consequently, this cooling method has the unique feature of delaying annihilation, which allows us to preserve a larger number of Ps atoms while cooling the ensemble. Furthermore, the estimate of the cooling laser intensity suggests that cooling is driven in the strongly saturated regime. Starting from a colder source at 150 K [39] and adding a second cooling stage with a narrower spectral bandwidth set closer to resonance will allow us to reach the recoil velocity in 22 cooling cycles (∼140 ns). Alternatively, coherent laser cooling [40,41] may be adapted to the positronium case. Ps laser cooling opens the door to an entirely new range of important fundamental studies, including precision spectroscopy, Bose-Einstein condensation of antimatter, and tests of the equivalence principle with a purely leptonic matter-antimatter system.

The authors are grateful to P. Yzombard, C. Zimmer, and O. Khalidova for early contributions to this activity, to L. Cabaret for the development of the 1^3S-2^3P laser, and to Dr. S. Cialdi for the original development of the 1^3S-3^3P laser. This work was supported by the ATTRACT program under Grant Agreement No. EU8-ATTPRJ (project O–Possum II); Istituto Nazionale di Fisica Nucleare; European Union's Horizon 2020 research and innovation programme under the Marie Skłodowska-Curie Grant Agreement No. 754496, FELLINI, and No. 748826, ANGRAM; the CERN Fellowship program and the CERN doctoral student program; the EPSRC of UK under Grant No. EP/X014851/1; Research Council of Norway under Grant Agreement No. 303337 and NorCC; NTNU doctoral program; the Research University Excellence Initiative of Warsaw University of Technology via the strategic funds of the Priority Research Centre of High

Energy Physics and Experimental Techniques; the IDUB POSTDOC program; the Polish National Science Centre under Agreements No. 2022/45/B/ST2/02029 and No. 2022/46/E/ST2/00255, and by the Polish Ministry of Education and Science under Agreement No. 2022/WK/06; Marie Skłodowska-Curie Innovative Training Network Fellowship of the European Commission's Horizon 2020 Programme (No. 721559 AVA); Wolfgang Gentner Programme of the German Federal Ministry of Education and Research (Grant No. 13E18CHA); European Research Council under the European Unions Seventh Framework Program FP7/2007-2013 (Grants No. 291242 and No. 277762); the European Social Fund within the framework of realizing the project, in support of intersectoral mobility and quality enhancement of research teams at Czech Technical University in Prague (Grant No. CZ.1.07/2.3.00/30.0034).

*Corresponding author: brienaec@liverpool.ac.uk
†Corresponding author: antoine.camper@fys.uio.no
‡Corresponding author: ruggero.caravita@cern.ch

[1] M. Deutsch, Evidence for the formation of positronium in gases, Phys. Rev. **82**, 455 (1951).
[2] D. B. Cassidy, P. Crivelli, T. H. Hisakado, L. Liszkay, V. E. Meligne, P. Perez, H. W. K. Tom, and A. P. Mills, Positronium cooling in porous silica measured via Doppler spectroscopy, Phys. Rev. A **81**, 012715 (2010),
[3] M. Antonello, A. Belov, G. Bonomi, R. S. Brusa, M. Caccia, A. Camper, R. Caravita, F. Castelli, D. Comparat, G. Consolati *et al.* (AEgIS Collaboration), Rydberg-positronium velocity and self-ionization studies in a 1T magnetic field and cryogenic environment, Phys. Rev. A **102**, 013101 (2020).
[4] S. Mariazzi *et al.* (AEgIS Collaboration), High-yield thermalized positronium at room temperature emitted by morphologically tuned nanochanneled silicon targets, J. Phys. B **54**, 085004 (2021).
[5] M. S. Fee, A. P. Mills, S. Chu, E. D. Shaw, K. Danzmann, R. J. Chichester, and D. M. Zuckerman, Measurement of the positronium $1^3S_1 - 2^3S_1$ interval by continuous-wave two-photon excitation, Phys. Rev. Lett. **70**, 1397 (1993).
[6] M. S. Fee, S. Chu, A. P. Mills, R. J. Chichester, D. M. Zuckerman, E. D. Shaw, and K. Danzmann, Measurement of the positronium $1^3S_1 - 2^3S_1$ interval by continuous-wave two-photon excitation, Phys. Rev. A **48**, 192 (1993).
[7] E. P. Liang and C. D. Dermer, Laser cooling of positronium, Opt. Commun. **65**, 419 (1988).
[8] W. D. Phillips, Nobel Lecture: Laser cooling and trapping of neutral atoms, Rev. Mod. Phys. **70**, 721 (1998).
[9] T. Kumita, T. Hirose, M. Irako, K. Kadoya, B. Matsumoto, K. Wada, N. N. Mondal, H. Yabu, K. Kobayashi, and M. Kajita, Study on laser cooling of ortho-positronium, Nucl. Instrum. Methods Phys. Res., Sect. B **171**, 1527 (2002).
[10] D. B. Cassidy, H. W. K. Tom, and A. P. Mills, Fundamental physics with cold positronium, AIP Conf. Proc. **1037**, 66 (2008).
[11] D. B. Cassidy, Experimental progress in positronium laser physics, Eur. Phys. J. D **72**, 53 (2018).
[12] G. S. Adkins, D. B. Cassidy, and J. Pérez-Rios, Precision spectroscopy of positronium: Testing bound-state QED theory and the search for physics beyond the Standard Model, Phys. Rep. **975**, 1 (2022).
[13] C. Amsler *et al.* (Particle Data Group), Review of particle physics, Phys. Lett. B **667**, 101 (2008).
[14] S. G. Karshenboim, Positronium, antihydrogen, light, and the equivalence principle, J. Phys. B **49**, 144001 (2016).
[15] M. Charlton, Antihydrogen production in collisions of antiprotons with excited states of positronium, Phys. Lett. A **143**, 143 (1990).
[16] C. Amsler *et al.* (AEgIS Collaboration), Pulsed production of antihydrogen, Commun. Phys. **4**, 19 (2021).
[17] D. Krasnický, R. Caravita, C. Canali, and G. Testera, Cross section for Rydberg antihydrogen production via charge exchange between Rydberg positroniums and antiprotons in a magnetic field, Phys. Rev. A **94**, 022714 (2016).
[18] P. M. Platzman and A. P. Mills, Possibilities for Bose condensation of positronium, Phys. Rev. B **49**, 454 (1994).
[19] A. P. Mills, Jr, in *Physics with Many Positrons* (IOS Press, Amsterdam and SIF, Bologna, 2010).
[20] H. K. Avetissian, A. K. Avetissian, and G. F. Mkrtchian, Self-Amplified Gamma-Ray Laser on Positronium Atoms from a Bose-Einstein Condensate, Phys. Rev. Lett. **113**, 023904 (2014).
[21] K. Yamada *et al.*, Theoretical analysis and experimental demonstration of a chirped pulse-train generator and its potential for efficient cooling of positronium, Phys. Rev. Appl. **16**, 014009 (2021).
[22] K. Shu, X. Fan, T. Yamazaki, T. Namba, S. Asai, K. Yoshioka, and M. Kuwata-Gonokami, Study on cooling of positronium for Bose–Einstein condensation, J. Phys. B **49**, 104001 (2016).
[23] S. Mariazzi, P. Bettotti, S. Larcheri, L. Toniutti, and R. S. Brusa, High positronium yield and emission into the vacuum from oxidized tunable nanochannels in silicon, Phys. Rev. B **81**, 235418 (2010).
[24] S. Aghion *et al.* (AEgIS Collaboration), Positron bunching and electrostatic transport system for the production and emission of dense positronium clouds into vacuum, Nucl. Instrum. Methods Phys. Res., Sect. B **362**, 86 (2015).
[25] C. Amsler *et al.* (AEgIS Collaboration), Velocity-selected production of 2^3S metastable positronium , Phys. Rev. A **99**, 033405 (2019).
[26] K. P. Ziock, C. D. Dermer, R. H. Howell, F. Magnotta, and K. M. Jones, Optical saturation of the $1^3S - 2^3P$ transition in positronium, J. Phys. B **23**, 329 (1990).
[27] C. Zimmer, P. Yzombard, A. Camper, and D. Comparat, Positronium laser cooling in a magnetic field, Phys. Rev. A **104**, 023106 (2021).
[28] D. B. Cassidy, T. H. Hisakado, H. W. K. Tom, and A. P. Mills, Laser excitation of positronium in the Paschen-Back regime, Phys. Rev. Lett. **106**, 173401 (2011).
[29] A. Camper *et al.* (AEḡIS Collaboration)(to be published).
[30] M. Hemmer, Y. Joly, L. Glebov, M. Bass, and M. Richardson, Volume Bragg Grating assisted broadband tunability and spectral narrowing of Ti:Sapphire oscillators, Opt. Express **17**, 8212 (2009).

[31] D. B. Cassidy, T. H. Hisakado, H. W. K. Tom, and A. P. Mills, Jr., Efficient production of Rydberg positronium, Phys. Rev. Lett. **108**, 043401 (2012).

[32] S. Aghion *et al.* (AEgIS Collaboration), Laser excitation of the $n = 3$ level of positronium for antihydrogen production, Phys. Rev. A **94**, 012507 (2016).

[33] D. Nowicka *et al.* (AEgIS Collaboration), Control system for ion Penning traps at the AEgIS experiment at CERN, J. Phys. Conf. Ser. **2374**, 012038 (2022).

[34] M. Volponi, S. Huck *et al.* (AEgIS Collaboration) CIRCUS: an autonomous control system for antimatter, atomic and quantum physics experiments, EPJ Quantum Technol. (2024).

[35] D. B. Cassidy, S. H. M. Deng, H. K. M. Tanaka, and A. P. Mills Jr., Single shot positron annihilation lifetime spectroscopy, Appl. Phys. Lett. **88**, 194105 (2006).

[36] S. Aghion *et al.* (AEgIS collaboration), Producing long-lived 2^3S positronium via 3^3P laser excitation in magnetic and electric fields, Phys. Rev. A **98**, 013402 (2018).

[37] F. Pedregosa, G. Varoquaux, A. Gramfort, V. Michel, B. Thirion, O. Grisel, M. Blondel, P. Prettenhofer, R. Weiss, V. Dubourg *et al.*, Scikit-learn: Machine Learning in Python, J. Mach. Learn. Res. **12**, 2825 (2011), https://dl.acm.org/doi/10.5555/1953048.2078195.

[38] D. B. Cassidy, T. H. Hisakado, H. W. K. Tom, and A. P. Mills, Positronium hyperfine interval measured via saturated absorption spectroscopy, Phys. Rev. Lett. **109**, 073401 (2012).

[39] S. Mariazzi, P. Bettotti, and R. S. Brusa, Positronium cooling and emission in vacuum from nanochannels at cryogenic temperature, Phys. Rev. Lett. **104**, 243401 (2010).

[40] C. Corder, B. Arnold, and H. Metcalf, Laser cooling without spontaneous emission, Phys. Rev. Lett. **114**, 043002 (2015).

[41] J. P. Bartolotta, M. A. Norcia, J. R. K. Cline, J. K. Thompson, and M. J. Holland, Laser cooling by sawtooth-wave adiabatic passage, Phys. Rev. A **98**, 023404 (2018).